Improved algorithm for 3D non-contrast pulmonary MRA

Chia-Ling Chang[1], Tzu-Cheng Chao[1,2], Maria Alejandra Duràn-Mendicuti[3], Ming-Ting Wu[4,5], and Bruno Madore[3]

[1]Department of Computer Science and Information Engineering, National Cheng-Kung University, Tainan, Taiwan, [2]Institute of Medical Informatics, National Cheng-Kung University, Tainan, Taiwan, [3]Department of Radiology, Brigham and Women's Hospital, Harvard Medical School, Boston, Massachusetts, United States, [4]Department of Radiology, Kaohsiung Veteran General Hospital, Kaohsiung, Taiwan, [5]School of Medicine, National Yang-Ming University, Taipei, Taiwan

Target Audience: Radiologists and researchers interested in non-contrast enhanced pulmonary angiography.

Purpose: Risks for nephrogenic systemic fibrosis have led to renewed interest in non-contrast enhanced (non-CE) angiography methods. In an emergency room environment, a reliable non-CE pulmonary MRA method could allow patients with suspected pulmonary embolism (PE) and contra-indication for CT angiography to be better cared for. Such method, utilizing flow related enhancement (FRE) as endogenous contrast, was introduced in Ref [1]; it included a dual sagittal slab excitation scheme to image both lungs at once and was ECG-gated to detect pulsatility and help distinguish veins from arteries. The whole volume of the lungs gets covered using several slabs (see Fig. 1), and the main weakness of the approach may be the presence of signal discontinuities at the boundaries between slabs. These discontinuities are caused by the FRE effect itself, whereby blood signal tends to be brighter at the entry point into the slab than at its exit point, but also from inconsistencies in the positioning of the anatomy from one breath-hold to the next. The ability to perform meaningful projections and 3D reformatting of the acquired 3D volume is greatly diminished by the presence of such discontinuities. The main purpose of the present work is to minimize signal discontinuities at the boundaries between slabs, without adversely affecting the underlying vascular signal.

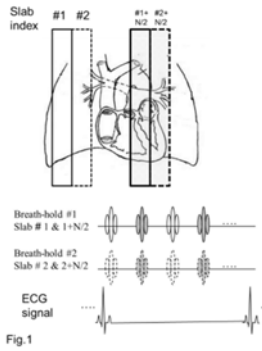

Fig.1

Methods: A non-rigid registration method tailored to the present application was developed here to mitigate the effect of inconsistent breath-holding positions. It is well known that the position of the diaphragm during breath-holding can be linearly correlated with vessel position[2,3]. We propose a registration algorithm that exploits available prior knowledge, both about the slab sampling scheme used here (Fig. 1) and about expected correlations between diaphragm motion and vessel motion:

The shape of the chest cavity was detected by region growing and finite difference filtering. The location of the upper edge, just under the clavicle, was recorded as y_i^{up}, where i is the slab index. y_i^{up} served as an anchor point for later image stretching. The position of the lower edge, the diaphragm, was also detected and the distance between the upper and lower edge was recorded as D_i. The outline of the diaphragm was saved as $S_i(x,y,z)$, with x, y and z the voxels index along the A-P, S-I and R-L directions, respectively. $S_i(x,y,z)$ is not expected to be well captured near the heart for lack of a clear signal edge there, but it becomes much more reliable away from the main trunk. The dual slab excitation scheme from Fig. 1 ensures that any slab located near the main trunk gets imaged at the same time as another slab further away, so that the latter may be used to provide the required motion information. The displacement of the diaphragm was calculated by minimizing signal discrepancies of shifted landmarked images:

$$\mathrm{Argmin}_{\Delta y_{i+\frac{1+k*N_v}{2}}} \sum_x \left| s_{i+\frac{+k*N_v}{2}}(x,y,z_{last}) - s_{i+\frac{1+k*N_v}{2}}\left(x, y+\Delta y_{i+\frac{N_v}{2}+1}, z_{first}\right)\right|^2 \quad for\ k=0\ or\ 1$$

Displacements are mostly expected to occur along S/I, and for this reason only shifts along y are considered in the expression above. The first pair of slabs provided a reference location for the registration, leading to $\Delta y_1 = \Delta y_{N_v/2+1} = 0$. Displacement for two simultaneously-acquired slabs, Δy_i and $\Delta y_{i+N_v/2}$, should be very similar; whenever large discrepancies were observed one of the two slabs would typically be located near the heart. In such cases the value found for the slab furthest away from the central trunk was considered more reliable and was automatically picked to represent both slabs. Once all displacement values had been found they were fed into a linear stretching model whereby each slab image $I_i(x,y,z)$ was deformed by:

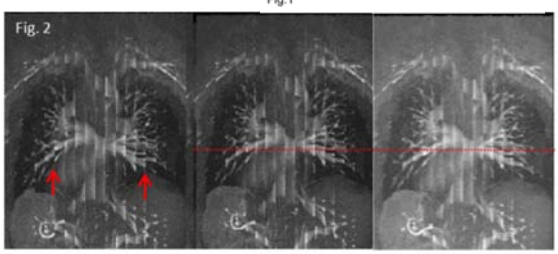
(a) No correction (b)Elastic Registration (c)Elastic Registration + Intensity Correction

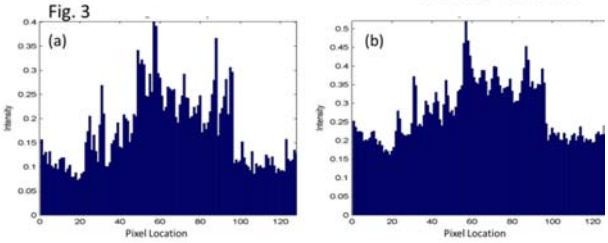

Fig. 3

$$I'_{i+k*\frac{N_v}{2}}(x,y,z) = I_{i+k*\frac{N_v}{2}}\left(x, y^{up}_{i+k*\frac{N_v}{2}} + \frac{\left(D_{i+k*\frac{N_v}{2}} + \sum_{i=1}^{\frac{N_v}{2}} \Delta y_{i+k*\frac{N_v}{2}}\right)}{D_{i+k*\frac{N_v}{2}}}\left(y - y^{up}_{i+k*\frac{N_v}{2}}\right), z\right), for\ \ k=0\ or\ 1.$$

Following the image registration, intensity correction could be performed to mitigate the variations caused by FRE between the entry point of one slab and the exit point of its neighbor. The intensity correction is a combination of two separate strategies: a half-pixel shift interpolation along z, and a power weighting adjustment. By shifting the pixel grid along z by a half-pixel, the signal transitions fall halfway in-between slices rather than at one given slice, thus smoothing the signal change. The half-pixel shift was implemented as a linear phase ramp in Fourier space along k_z, and thus did not degrade in any way the spatial resolution of the underlying object. As a further correction, a power weighting also helped reduce discontinuities. When combining both strategies, the corrected signal was obtained from the original (registered) results as $I_i''(x,y,z) = I_i'(x,y,z+0.5)^p$. A power setting of 0.6<p<0.8 was empirically chosen here.

Seven healthy volunteers were imaged on a 1.5T system following informed consent (3D spoiled gradient-echo sequence, TE/TR = 1.7/6.8 ms , 8 slices per slab, 16 to 18 slabs needed to cover the chest, 8 to 9 breath-holds per exam).

Results: Maximal intensity projections in the coronal plane are shown in Fig. 2. While slab-to-slab discontinuities would not be conspicuous in a sagittal projection, they are maximally visible in axial and coronal projections. Discontinuities for vessels (red arrows) and liver can be readily noticed in Fig. 2a. Introducing the elastic deformation scheme described above nearly eliminated all displacement problems at boundaries, as seen in Fig. 2b. Further adding the proposed intensity correction helped alleviate the stairway artifact caused by the flow-related enhancement, but did not eliminate it, as can be seen in Fig. 2c. In Fig. 3, the signal profiles for the indicated sections were plotted for comparison. It can be noticed that the variation within the vessel region becomes smaller after intensity correction (Fig. 3b) while the background grey level remains low even in Fig. 3c.

Discussion and Conclusion: There is a clinical need for a reliable non-CE pulmonary MRA method, for patients with suspected PE and contra-indication to CT angiography. Images cannot be expected to be as esthetically appealing as in CE MRA, but must be sufficiently good to detect PE. A reasonable approach was introduced in Ref. [1] whose main drawback may have been the presence of discontinuities at the junction between slabs. The strategies presented here were successful in attenuating the negative effects of this main weak point.

Reference: [1] T.C. Chao, et al, ISMRM 2012, p.3900 [2] P. G. Danias, et al. AJR, 1999, p.1061. [3] K. Nehrke, et al. Radiology, 2001, p810

Support is acknowledged from NSC grants: 100-2218-E-006-038-MY2 and 102-2221-E-006-017 and NIH grants: R01CA149342, R01EB010195 and P41EB015898.